Journal of Atmospheric and Solar-Terrestrial Physics 129 (2015) 6–12

Contents lists available at ScienceDirect

Journal of Atmospheric and Solar-Terrestrial Physics

journal homepage: www.elsevier.com/locate/jastp

Extracting planetary waves from geomagnetic time series using Empirical Mode Decomposition

Dennis Frühauff [a,*], Karl-Heinz Glassmeier [a], Michael Lockwood [b], Daniel Heyner [a]

[a] Institut für Geophysik und extraterrestrische Physik, Technische Universität Braunschweig, Mendelssohnstr. 3, 38106 Braunschweig, Germany
[b] Meteorology Department, University of Reading, Reading, Berkshire, United Kingdom

ARTICLE INFO

Article history:
Received 13 October 2014
Received in revised form
30 March 2015
Accepted 5 April 2015
Available online 6 April 2015

Keywords:
Empirical Mode Decomposition
Planetary waves
Rossby wave
Geomagnetic jerks
Solar cycle

ABSTRACT

Empirical Mode Decomposition is presented as an alternative to traditional analysis methods to decompose geomagnetic time series into spectral components. Important comments on the algorithm and its variations will be given. Using this technique, planetary wave modes of 5-, 10-, and 16-day mean periods can be extracted from magnetic field components of three different stations in Germany. In a second step, the amplitude modulation functions of these wave modes can be shown to contain significant contribution from solar cycle variation through correlation with smoothed sunspot numbers. Additionally, the data indicate connections with geomagnetic jerk occurrences, supported by a second set of data providing reconstructed near-Earth magnetic field for 150 years. Usually attributed to internal dynamo processes within the Earth's outer core, the question of who is impacting whom will be briefly discussed here.

1. Introduction

Planetary waves, also known as free, large-scale Rossby waves, are motions of the neutral gas in the Earth's atmosphere. Their theoretical prototype can be shown to be the solution of the set of equations describing isothermal atmospheres (Hirota and Hirooka, 1984; Hirooka and Hirota, 1985; Salby, 1984). It has been previously suggested that the observed atmospheric oscillations have an influence on geomagnetic variations due to a resulting dynamo action in the E-layer of the ionosphere (Forbes and Leveroni, 1992; Parish et al., 1994). Kohsiek et al. (1995) characterize their effect by three essential factors: 1. the ionization of the upper atmosphere (resulting from UV and X-ray radiation from the sun); 2. wind systems; 3. the permanent geomagnetic field.

Traditionally, evidence for the presence of planetary wave modes in geomagnetic time series is found using power spectral density estimates. The three most prominent modes, commonly referred to as 5-day, 10-day, and 16-day wave, feature approximate periods of $T \approx 4.5$–6.2 days, $T \approx 7.5$–12 days, and $T \approx 11$–21 days, respectively (Salby, 1984). As conventional Fourier analysis is constrained to stationary data and linear processes with harmonic basis functions, the application of newer methods can provide additional insight in the characteristics of planetary wave modes. Jarvis (2006) has used Short-Time Fourier Transform and Wavelet Transform to detect planetary wave modes. Here, we suggest Empirical Mode Decomposition (EMD), a spectral decomposition method working in the time domain, serving as a tool to extract these modes from geomagnetic variations and characterize their modulation. This technique has already been shown to be successful: Coughlin and Tung (2004) have used EMD to extract the 11-year solar cycle from stratospheric data, Roberts et al. (2007) extracted 60-year periodicities from length of day observations, Jackson and Mound (2010) found evidence for persistent internal time scales due to the outer core dynamo in geomagnetic data, Panovska et al. (2013) have used EMD and other techniques to search for periodicities of up to several thousands of years in Holocene sediment magnetic records.

Despite proving to be an effective algorithm, there are certain issues one needs to be aware of while using Empirical Mode Decomposition. In the present work we will discuss some of these before we employ EMD to extract and characterize planetary wave modes in geomagnetic time series. The paper is organized as follows: Section 2 gives a brief overview of the data used for the analysis. Section 3 will introduce Empirical Mode Decomposition as a procedure, and discuss some of the related difficulties. Section 4 will consider the extraction and characterization of planetary wave modes. Finally, discussion and outlook will be given in

* Corresponding author.
E-mail address: d.fruehauff@tu-bs.de (D. Frühauff).

http://dx.doi.org/10.1016/j.jastp.2015.04.002
1364-6826/

Section 5.

2. Data and preprocessing

With planetary wave modes being very pronounced in mid-latitudes, geomagnetic time series from three different stations in Germany are used. The three observatories are located in Niemegk (NGK), Wingst (WNG), and Fürstenfeldbruck (FUR). An overview is given in Table 1. Following the study of Kohsiek et al. (1995) the aim is to show that EMD can provide similar results. In a later study, globally distributed data should be analyzed as well. The original time series feature hourly values of *X*-,*Y*-, and *Z*-components of the geomagnetic field. In a first step, these data are reduced to daily means. Following traditional suggestions, the data are then interpolated linearly when there are missing values (Kohsiek et al., 1995). Unfortunately, all records contain significant gaps of up to a few years in length (e.g., during World War 2 for NGK data). Therefore, it is not possible to use the full-length data for the analysis. Although EMD itself does not appear to be highly susceptible to non-equidistant sampling, formal frequency and period estimation is. As a consequence, the intervals that can be used are reduced to 1947/07/29–2013/12/31 (NGK), 1968/09/01–2012/12/31 (WNG), and 1946/08/02–2011/12/31 (FUR). From these intervals H-, D-, I-, and Z-components of the magnetic field as defined in Finlay et al. (2010) will be computed to be used in the analysis.

3. Empirical Mode Decomposition

Empirical Mode Decomposition has been introduced by Huang et al. (1998) as an effective algorithm to decompose time series into the so-called Intrinsic Mode Functions (IMFs, here referred to as "modes" to avoid any connotation with the interplanetary magnetic field). These modes form a (quasi-)orthogonal[1] set of basis functions that is derived directly from the original data without *a priori* assumptions about their nature. Besides orthogonality of the total set of basis functions, each mode is required to meet two extra conditions: First, the number of extreme values and zero crossings differ at most by one. Second, the "local mean" value of the mode is zero (Huang et al., 1998).

3.1. Fundamentals and spectral analysis

The basic algorithm of EMD can be described as follows:

1. Start with a discrete time series $x(t)$ with sampling period T_s.
2. Compute all maximum (minimum) values of $x(t)$, perform cubic spline interpolation, $e_{\max}$ ($e_{\min}$), for these values.
3. Estimate the local mean of the time series as $m(t) = \frac{1}{2}(e_{\max} + e_{\min})$.
4. Subtract $m(t)$ from $x(t)$ and repeat the process with the resulting time series, beginning from Step 2, until a stopping criterion is reached.
5. When the stopping criterion is met, the first mode, $C_1(t)$, is found. Subtract this mode from the original signal and repeat the whole process for the residual.
6. The procedure can be stopped when the signal does not contain enough extreme values to perform interpolation. This residual can be regarded as the global trend, $R(t)$, of the time series.

[1] The term "quasi-orthogonal" refers to orthogonality in a numerical sense. No mathematical theory has been derived for EMD to this day (Deléchelle et al., 2005).

Table 1
Information on the observatories.

Station	Location	Time interval
NGK	52.08°N, 12.70°E	1890–2013
WNG	53.75°N, 9.07°E	1943–2011
FUR	48.17°N, 11.28°E	1940–2011

By definition of the procedure, the original time series can be represented as

$$x(t) = \sum_{i=1}^{n} C_i(t) + R(t), \tag{1}$$

with n being the number of extracted basis functions.

EMD defines oscillations as the succession of extreme values and, consequently, permits modulation in its modes. It is therefore possible to perform time-dependent frequency and amplitude analysis. As suggested by Huang et al. (1998) this can be done using Hilbert analysis and transforming the independent modes into analytical signals. An analytical signal, $z(t)$, can be defined as

$$z(t) = x(t) + \mathrm{i}y(t) = x(t) + \mathrm{i}\mathcal{H}\{x(t)\}, \tag{2}$$

with $\mathcal{H}\{x(t)\}$ being the discrete Hilbert transform of $x(t)$ (Farnbach, 1975; Glassmeier, 1980). Using the amplitude and phase functions,

$$A(t) = \sqrt{x^2(t) + y^2(t)}, \tag{3}$$

$$\Phi(t) = \arctan\frac{y(t)}{x(t)}, \tag{4}$$

and the instantaneous frequency function

$$\omega(t) = \frac{d}{dt}\Phi(t), \tag{5}$$

the original time series can be represented as

$$x(t) = \sum_{i=1}^{n} A_i(t)\exp\left(\mathrm{i}\int \omega_i(t)\,dt\right). \tag{6}$$

The decomposition performed by the EMD algorithm can therefore be regarded as a generalization of the traditional Fourier analysis. Still, Empirical Mode Decomposition lacks a theoretical basis (Deléchelle et al., 2005).

3.2. Algorithmic obstacles

There are two main issues to be addressed when applying Empirical Mode Decomposition: First, the implementation of boundary conditions (or boundary extension), and second, the selection of an appropriate stopping criterion. Several different versions of boundary conditions and stopping criteria have been developed in the past. While all different methods do perform well (under certain conditions), the overall decompositions are sensitive to the choice of algorithmic variations. Unfortunately, few working groups mention their specific method in their publications. In order to be able to understand and reproduce results, it is yet absolutely necessary to reveal both stopping criterion and boundary extension method to the interested reader. In the present work, the amplitude ratio stopping criterion proposed by Rilling et al. (2003) is implemented using the default set of threshold values. The boundary extension method is based on linear extrapolation as suggested by Wu and Huang (2009).

Table 2
Comparison of the mean resulting periods using different sampling periods for data between 1962/07/01 and 2012/07/01 of NGK, dH/dt-Component.

Mode #	$\langle T \rangle$ (yrs) $T_s = 1$ yrs	$\langle T \rangle$ (yrs) $T_s = 1$ mo	$\langle T \rangle$ (yrs) $T_s = 1$ d
1	4.14	0.39	0.01
2	11.00	0.76	0.02
3	Trend	1.32	0.03
4		2.51	0.04
5		5.01	0.06
6		12.71	0.11
7		53.17	0.16
8		Trend	0.30
9			0.49
10			0.98
11			2.01
12			3.57
13			7.21
14			12.73
15			25.71

3.3. Expected number of basis functions

As shown by Flandrin (2004) EMD acts as a dyadic filtering structure in the presence of Gaussian noise within the signal. Therefore, the mean frequency of the basis functions tends to decrease by a factor of 2 for increasing the mode's ordinal number. Still, frequency overlapping can occur, especially in the case of high sampling frequencies or large data sets. It can easily be verified that the number of basis functions, n, that can be expected to result from the decomposition is approximately

$$n \leq \log_2 N, \tag{7}$$

with the number of data points, N, available. As N can be regarded as a function of both sampling frequency and length of time interval, one needs to carefully choose these two parameters in order to derive specific results and avoid extensive frequency overlap.

To demonstrate this effect an EMD analysis comparing the mean periods of the same data set (NGK data) for daily, monthly, and yearly values is performed. The results are given in Table 2.

As indicated, the frequency resolution is highly dependent on the sampling period (the number of data points). Therefore, when looking for a specific frequency in a signal it is advisable to choose T_s accordingly. Generally, and, as already indicated by Huang et al. (1998), it is recommended to check the set of modes for significance, e.g., to identify modes with significant amplitude. Having a small sampling time almost certainly will lead to a subset of modes with negligible amplitude, which should not be considered relevant.

All three decompositions in Table 2 show components with mean periods of approximately 12 years.[2] On the other hand, the decompositions featuring monthly and yearly values contain modes with periods of about 5 years, whereas EMD does not extract such a component from daily-sampled data of the same interval. Still, this mode might be contained in its two neighboring periods 3.57 years and 7.21 years, being buried by the effect of oversampling and frequency overlap. As an advice, one should choose the sampling frequency as high as necessary and as low as possible to produce acceptable results, e.g., being interested in signals featuring monthly periods, there is no need to analyze daily sampled data, nor will it make sense to go for yearly averaged data.

[2] Typically, this period is associated with the solar Schwabe cycle, representing an external disturbance in the geomagnetic field (Coughlin and Tung, 2004). The possible meaning of periods will be examined in Section 4.

4. Extraction and characterization

4.1. Direct analysis of geomagnetic data

Typically, the analysis of geomagnetic time series is done using the first (or second) time derivatives of the original data (Roberts et al., 2007; Jackson and Mound, 2010). This preprocessing step is done to ensure that weak frequency components are not dominated by large data trends that are present in the time series. While frequency information is thereby pronounced and conserved, this involves the loss of all amplitude information. However, such a procedure lacks key possibilities provided by EMD and Hilbert transform, namely, to study amplitude and frequency modulation.

As an alternative to this approach, detrending of the original time series using the International Geomagnetic Reference Field (IGRF) model is suggested. The model description and an online calculation tool are given in Finlay et al. (2010). An example representation can be seen in Fig. 1 (yearly averaged data).

As expected, the remaining time series is not dominated by a major trend. The remaining offset probably results from remanent crustal magnetization, and small external contributions arising from non-zero external background field not modeled by IGRF (Lühr and Maus, 2010). This offset is of the same order as expected variations in the original time series. The resulting decomposition of the detrended time series is shown in Fig. 2. As even the remainder, C_4, shows an oscillating behavior, all four components can be assigned with a mean period. These are $\{3.7 \pm 1.3, 7.8 \pm 1.4, 18.6 \pm 5.8, 61.0 \pm 9.0\}$ years. As frequency estimation using Hilbert analysis is very sensitive to the sampling period of the time series, the mean periods of these modes are found by averaging over manually traced maxima and minima spacings in the data. First and interestingly, no noticeable 11-year component is found in this decomposition. Such a period would indicate the presence of a Schwabe-like cycle in the trend-reduced time series. It is commonly agreed that the Schwabe cycle does not feature an exact 11-year period, but varies in length between 9 and 14 years (Benestad, 2005). 11-year periods are nevertheless seen in observatory series (Love and Rigler, 2014). Therefore, its footprint might still be in the data, buried in the second and third component of the decomposition. This is supported by the fact that, by using different lengths the decomposition will be altered by the specific data

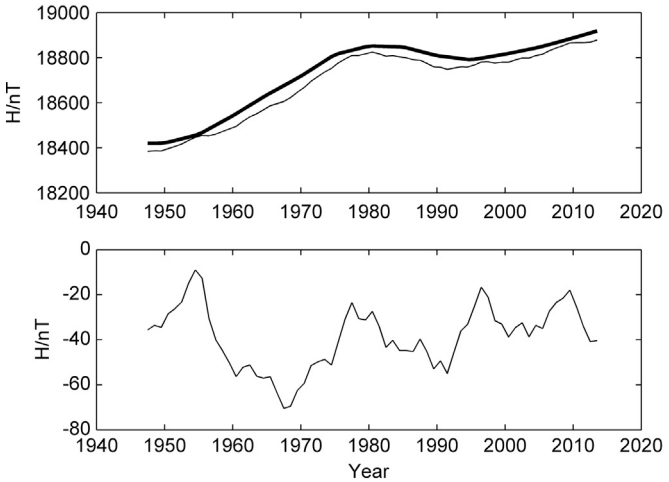

Fig. 1. H-component of NGK-data (upper panel, thin line) and IGRF model data (thick line) and data after detrending using the reference field (lower panel).

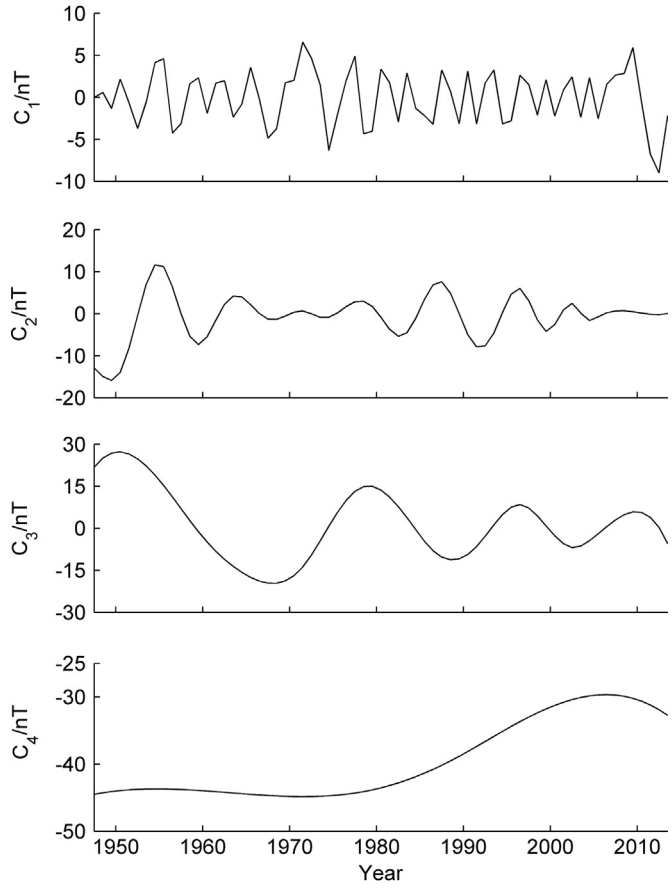

Fig. 2. The four extracted modes from the detrended NGK data (yearly values). Note different axis scaling.

interval used. The presence of a shorter (or longer) cycle will certainly influence the mean period calculated from the data set. Second, the 61-year component (C_4) indicates a long-term influence on the geomagnetic field. Traditionally, a period of about 60 years will immediately be recognized as a signal emanating from the Earth's interior (Jackson and Mound, 2010; Roberts et al., 2007). At this point, the same component might as well be of external origin, representing a Gleissberg-like cycle modulation (Feynman and Fougere, 1984; Feynman and Ruzmaikin, 2011). Further discussion of this separation problem will be given in the last section.

It should be noted that using IGRF is not the only possibility to remove modeled trends from geomagnetic time series. Smooth and spline-based internal field models such as COV-OBS (Gillet et al., 2013), or gufm1 (Jackson et al., 2000) should also provide good proxies for data detrending. Additionally, since IGRF is interpolated linearly on a 5-year grid, a smoothed spline fit to this model can as well improve results slightly here. The differences in the results are not expected to be large, though, especially for the short-period components. Therefore, no further intensification on this topic needs to be made here.

The primary aim of this work is the extraction and characterization of planetary wave modes using EMD. Therefore, daily mean values are now used in the analysis procedures. The illustration of the results will focus on NGK data, H-component. The investigation of the other data sets produces similar results.

As the characteristic timescales of planetary wave modes and data-dominating trends differ by several orders of magnitude, it is *not* necessary to manipulate the time series through artificial detrending procedures such as removing the IGRF. The first few mean periods and their related amplitudes that are produced when performing EMD on the (undetrended) NGK data are given in Table 3.

Fig. 3 displays the specific component of the H-component decomposition, C_{H5}, that can be related to a mean period of 5.6 days. Additionally, the estimation of the instantaneous frequency over time is shown. The values have been smoothed with a sliding average over 365 values. It can be visually verified that the instantaneous frequency lies within the expected interval for the 5-day planetary wave for over 90% of the time. Likewise, 10-day and 16-day planetary wave modes can be identified in the subsequent modes #3 and #4. The two corresponding modes are displayed in Fig. 3 as well, indicating very similar amplitude modulation.

4.2. Analysis of amplitude modulation functions

Since all three of the aforementioned components feature similar amplitude modulation, the discussion will be limited to the 5-day planetary wave mode. Analyzing any of these signals produces resembling results. To characterize this modulation, the analysis will be taken one step further by performing a second decomposition with EMD on the amplitude function of the 5-day planetary wave mode. Using Hilbert analysis the instantaneous amplitude function can be computed from the time series. As the characteristic timescales of the amplitude function appear to span several years, the daily sampled data are now reduced to yearly

Table 3
Comparison of the first extracted modes of H-, D-, I-, and Z-components of NGK data.

(a) Estimated mean periods of modes.				
#	$\langle T_H \rangle$ (d)	$\langle T_D \rangle$ (d)	$\langle T_I \rangle$ (d)	$\langle T_Z \rangle$ (d)
1	4.0	3.7	3.9	3.8
2	5.6	5.3	5.5	5.2
3	9.0	8.7	9.1	8.4
4	15.3	13.9	16.2	14.2
5	28.2	25.1	29.2	24.6
...	...	...	...	
(b) Amplitudes of modes.				
#	$\hat{A}_H$ (nT)	$\hat{A}_D$ (mrad)	$\hat{A}_I$ (mrad)	$\hat{A}_Z$ (nT)
1	46.1	1.3	0.8	30.3
2	48.1	0.9	1.0	18.3
3	30.9	0.8	0.8	24.0
4	31.1	0.9	0.6	30.1
5	24.3	0.5	0.5	12.9
...	...	...	...	

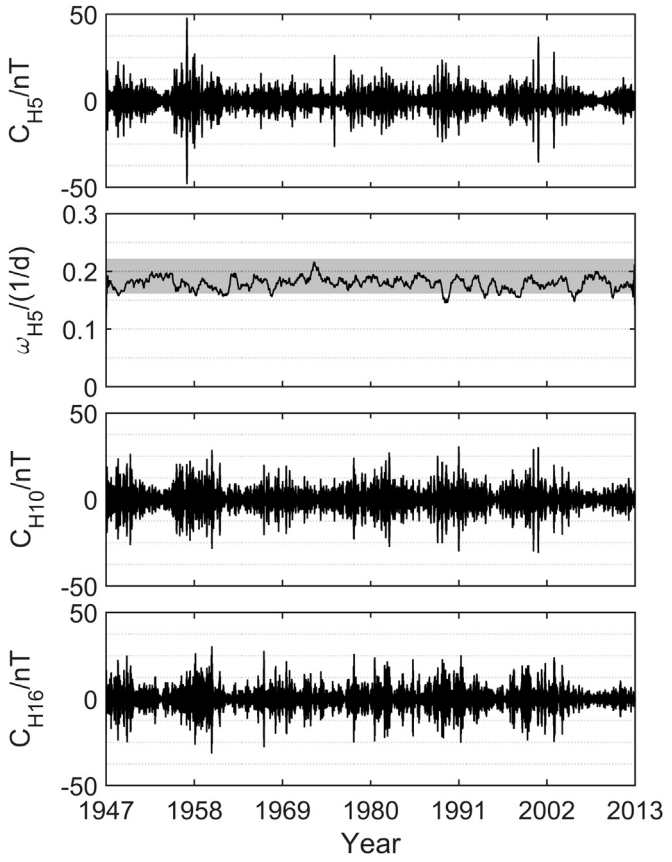

Fig. 3. Specific mode related to a mean period of 5.6 days of the H-component (upper panel). Estimation of the instantaneous frequency of this mode as calculated from Eq. (5) and frequency interval of the 5-day planetary wave (second panel, shaded area). The two lower panels additionally display the components containing the 10- and 16-day planetary waves for comparison.

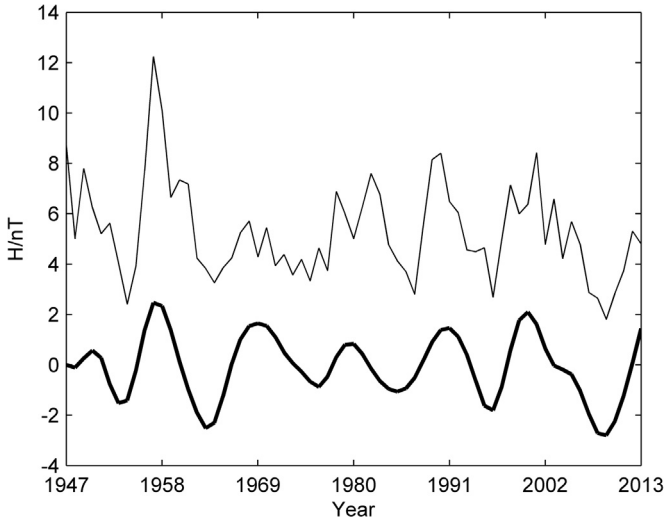

Fig. 4. The amplitude modulation of the extracted 5-day planetary wave (thin line) and the second mode contained in this signal with a mean period of approximately 10 years (thick line).

mean values. The decomposition results in three oscillating modes with estimated mean periods of $\{3.2 \pm 1.4, 10.1 \pm 2.4, 24.33 \pm 2.5\}$ years, and a long-term oscillating component with a period of roughly 52 years. All four components show similar peak-to-peak amplitudes of around 2 nT (Fig. 4).

As can be seen in Fig. 5, the 10-year component of the amplitude modulation shows very good correlation with the sunspot number. The sunspot data are sampled at daily intervals and smoothed by a sliding average over 365 values for visualization. After reducing the sunspot data to yearly averages the formal Pearson correlation coefficient, r, can be calculated to be $r \simeq 0.81$. On the other hand, the 8-year component derived directly from the H-component (shown as C_2 in Fig. 2) does not show relevant correlation with the sunspot number.

Interestingly, both the direct and the amplitude function decomposition feature components with mean periods of approximately 20 years, or, within the range of uncertainty, 22 years. A 22-year periodicity immediately reminds of the 22-year Hale cycle in sunspot variability (Hale and Nicholson, 1938). The imprint of a 22-year modulation in planetary wave amplitudes has been studied by Jarvis (2006) using wavelet analysis. In that study, no "Schwabe-like" component is found due to the application of an 11-year sliding average to the data. Still, the influence of the 11-year cycle on several atmospheric phenomena on Earth has been well studied (Labitzke and Matthes, 2003). However, it remains unclear how solar magnetic field polarity changes as suggested by Hale and Nicholson (1938) could have an influence on terrestrial dynamics as the solar wind tends to mix up polarity effects on its way to Earth.

Again, a long term oscillation with a period of about 52 years is found in the data. Naturally, characterizing signals with periods similar to the record length is not always reliable and one should be advised to be careful in this respect. Therefore, a clear relationship to internal or external creation of this effect cannot be carried out within the scope of this work. The physically meaningful interpretation of EMD components has already been found difficult in many occasions, especially, while being unsure of what exactly to look for (Huang et al., 1998).

5. Discussion and outlook

In a first step Empirical Mode Decomposition has been used as a tool to extract planetary wave signatures from geomagnetic variations. The influence of these large-scale atmospheric oscillations on the geomagnetic field depends on mechanical coupling mechanisms between non-conducting and conducting layers of the atmosphere, and ionospheric degree of ionization. Therefore, solar variability suggests itself as a possible main driver for the amplitude modulation of the magnetic signatures caused by planetary waves.

To analyze this relationship, a second step of EMD analysis was performed on the amplitude modulation function of the 5-day planetary wave mode extracted from geomagnetic observatory data. One of the resulting components shows good correlation with the smoothed sunspot number and may therefore be identified as a Schwabe-type modulation of the 5-day wave. Interestingly, a 11-year signal was not found directly in the time series of the H-component itself. It is expected that this 11-year signal is buried in its neighboring components.

The interpretation of the 24-year component remains difficult. Although a Hale-type modulation would feature a period of about 22 years, it is unclear how sunspot polarity can affect geomagnetic time series after being mixed up by solar wind turbulence.

Lastly, both in the original decomposition and in the decomposition of the amplitude modulation components with mean periods of roughly 50–60 years are found. Although 60-year oscillations are no longer identified as resonant torsional oscillations in the Earth's core as done by Jackson and Mound (2010) (the current estimate produces periods of about 6 years, Gillet et al., 2010), such slow signals are still considered to be related to the complex and nonlinear core dynamics. The existence of this

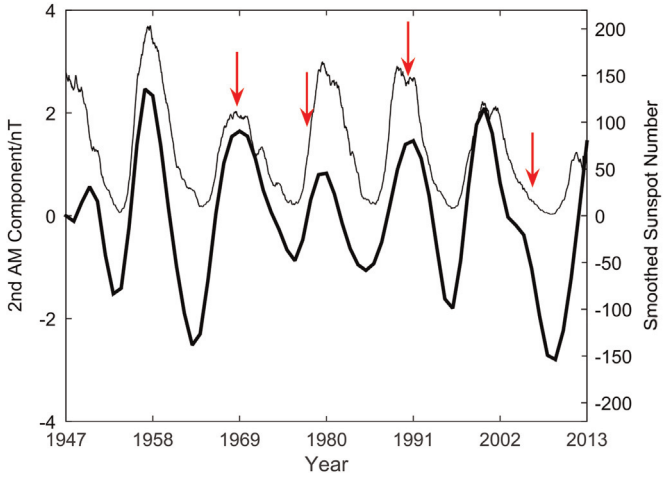

Fig. 5. The second mode contained in the amplitude modulation of the 5-day-wave (thick line) and the smoothed sunspot number (thin line). Arrows indicate positions of geomagnetic jerks in the years 1969, 1978, 1991, and 2007, respectively (Michelis, 2005; Pinheiro et al., 2011; Chulliat et al., 2010).

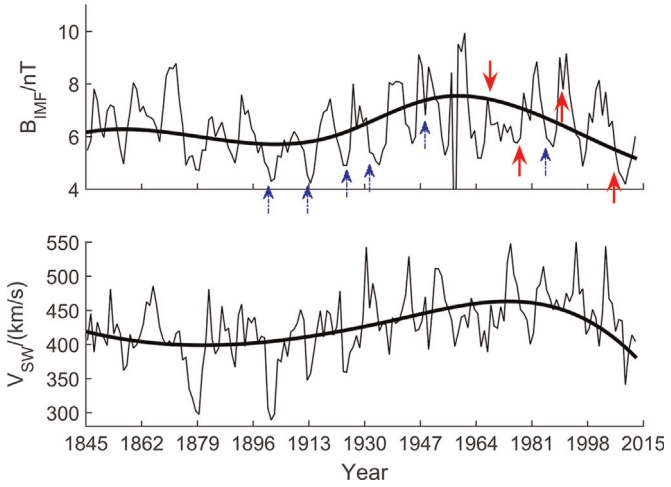

Fig. 6. Time series for near-Earth magnetic field, B_{IMF} (upper panel), and solar wind speed V_{SW} (lower panel), as derived by Lockwood et al. (2014). The thick curves show the EMD-derived trend of the time series. Arrows indicate geomagnetic jerk positions for 1901, 1913, 1925, 1932, 1949, 1969, 1978, 1986, 1991, 2007, respectively (Michelis, 2005; Pinheiro et al., 2011; Chulliat et al., 2010). Prominent jerks are highlighted in red (thick arrows), less prominent jerks in blue (thin, dashed arrows). (For interpretation of the references to color in this figure caption, the reader is referred to the web version of this paper.)

periodicity has been postulated before (Roberts et al., 2007), although recent theories suggest a different mechanism for the generation of these periods (Buffett, 2014). Either way, the generation of these signals is expected to be of internal origin. Still, the accurate separation of internal and external sources in the geomagnetic field variations is a difficult task even today. Thus, it is appropriate to ask whether the extracted components could instead be of external (solar-driven) origin. Lockwood et al. (2014) made an attempt to reconstruct near-Earth interplanetary wind speed, magnetic field, and open solar flux using different activity indices for the years 1845–2014.

By performing EMD analysis on the data for near-Earth solar wind speed and interplanetary magnetic field, components with mean periods listed in Table 4 are derived. The two original time series and the slowly oscillating EMD-derived trends are displayed in Fig. 6. As can be seen from the estimated mean periods, both time series contain modes of about 40–60 years in period and longer. Assuming that the method (Lockwood et al., 2014) used to derive the data is right, these long-scaled components, e.g., the 62-year signal, must be of *external* origin. In this case these periods can be associated with Gleissberg cycle-like modulations, which is especially the case for he 100-year signal contained in the interplanetary magnetic field, as already estimated long ago (Feynman and Fougere, 1984). On the other hand, if these periods were indeed of internal origin, the data derived by Lockwood et al. (2014) are shown to be contaminated by Earth's core dynamics.

A second interesting phenomenon can be seen when comparing global (and almost global) magnetic jerk events with different data. In Fig. 5 several of these events seem to coincide with prominent deviations of the amplitude modulation component of the 5-day planetary wave from the sunspot cycle. Similarly, considering Fig. 6, the jerk positions show some amount of correlation with the minimum values (and one maximum value) of the near-Earth interplanetary magnetic field derived by Lockwood et al. (2014). This behavior offers two possible solutions: 1. Geomagnetic jerks are in general interpreted as signatures that originate in the Earth's interior[3] (Malin and Hodder, 1982; Bloxham et al., 2002). If this is the case, the jerk events seem to influence the interplanetary magnetic field derived by Lockwood et al. (2014). The separation done in their work therefore needs to be reconsidered as jerks seem to have significant influence on the resultant data. Of course, this is a difficult task as the succession of jerks does not feature an *obvious* periodicity. 2. Assuming the applied method of deriving near-Earth data to be correct, i.e., B_{IMF} to be of external origin, such a correlation indicates an impact of external signals on the *existence* of geomagnetic jerks (The interplanetary magnetic field is possibly too weak to have measurable influence on in-Earth processes. Therefore, the solar wind speed could be the actual driver.). One would expect a significant time lapse between the trigger of such an event and the outcome in the geomagnetic field. Still, such a feedback system has already been examined in the case of planet Mercury (Glassmeier et al., 2007; Heyner et al., 2011). It should be mentioned that Légaut and Jault (2004) and Jault and Légaut (2005) proposed the possibility of external fields to induce currents in the outer core on more immediate timescales than those relying on dynamo feedback. This interaction mechanism might as well be considered in determining the relation between internal and external signatures in more detail given current electrical conductivity estimates of the mantle (Velímský and Finlay, 2011). At this point, the question clearly is: Who is impacting whom (and how)? As the primary aim of this work was to analyze planetary wave structures using EMD a deeper investigation of this topic cannot be carried out here. More detailed studies, ideally a full separation of any long-term observations of the geomagnetic field into its internal and external parts (Malin and Hodder, 1982; Duka et al., 2012) is necessary to allow for long-term variation analysis of the internal and external field contributions.

Table 4
Extracted mean periods of Lockwood data for near-Earth solar wind speed, V_{SW}, and magnetic field, B_{IMF}.

#	$\langle T_{VSW} \rangle$ (yrs)	$\langle T_{BIMF} \rangle$ (yrs)
1	3.1 ± 1.3	3.3 ± 1.5
2	7.7 ± 2.5	7.9 ± 2.5
3	13.5 ± 2.9	13.8 ± 5.5
4	23.1 ± 3.7	27 ± 11
5	62 ± 10	42.9 ± 8.9
6	≈ 180	≈ 100

[3] Some authors consider it possible that external signals *enhance* the effect of jerks. Still, they are expected to be of internal origin first (Alldredge, 1975, 1984).

Acknowledgments

The authors would like to thank the GFZ German Research Centre for Geosciences and the Max Planck Institute for Solar System Research Göttingen for providing relevant data sets. This work was financially supported by the German Ministerium für Wirtschaft und Energie and the German Zentrum für Luft- und Raumfahrt under Contract 50 OC 1403. Daniel Heyner was financially supported by the German Ministerium für Wirtschaft und Technologie and the German Zentrum für Luft- und Raumfahrt under Contract 50 QW 1101.

References

Alldredge, L.R., 1975. A hypothesis for the source of impulses in geomagnetic secular variations. J. Geophys. Res. 80, 1571–1578.
Alldredge, L.R., 1984. A discussion of impulses and jerks in the geomagnetic field. J. Geophys. Res.: Solid Earth 89, 4403–4412.
Benestad, R.E., 2005. A review of the solar cycle length estimates. Geophys. Res. Lett. 32.
Bloxham, J., Zatman, S., Dumberry, M., 2002. The origin of geomagnetic jerks. Nature 420, 65–68.
Buffett, B., 2014. Geomagnetic fluctuations reveal stable stratification at the top of the Earth's core. Nature 507, 484–492.
Chulliat, A., Thébault, E., Hulot, G., 2010. Core field acceleration pulse as a common cause of the 2003 and 2007 geomagnetic jerks. Geophys. Res. Lett. 37, 1–5.
Coughlin, K., Tung, K., 2004. 11-Year solar cycle in the stratosphere extracted by the empirical mode decomposition method. Adv. Space Res. 34 (January), 323–329.
Deléchelle, E., Lemoine, J., Niang, O., 2005. Empirical mode decomposition: an analytical approach for sifting process. IEEE Signal Process. Lett., 764–767.
Duka, B., De Santis, A., Mandea, M., Isac, A., Qamili, E., 2012. Geomagnetic jerks characterization via spectral analysis. Solid Earth 3, 131–148.
Farnbach, J.S., 1975. The complex envelope in seismic signal analysis. Bull. Seismol. Soc. Am. 65, 951–962.
Feynman, J., Fougere, P., 1984. Eighty-eight year periodicity in solar-terrestrial phenomena confirmed. J. Geophys. Res. 89, 3023–3027.
Feynman, J., Ruzmaikin, A., 2011. The Sun's strange behavior: Maunder minimum or Gleissberg cycle?. Solar Phys., 351–363.
Finlay, C.C., Maus, S., Beggan, C.D., Bondar, T.N., Chambodut, A., Chernova, T.A., Chulliat, A., Golovkov, V.P., Hamilton, B., Hamoudi, M., Holme, R., Hulot, G., Kuang, W., Langlais, B., Lesur, V., Lowes, F.J., Lühr, H., Macmillan, S., Mandea, M., McLean, S., Manoj, C., Menvielle, M., Michaelis, I., Olsen, N., Rauberg, J., Rother, M., Sabaka, T.J., Tangborn, A., Toffner-Clausen, L., Thébault, E., Thomson, A.W.P., Wardinski, I., Wei, Z., Zvereva, T.I., 2010. International geomagnetic reference field: the eleventh generation. Geophys. J. Int. 183, 1216–1230, URL: ⟨http://www.ngdc.noaa.gov/geomag-web/⟩.
Flandrin, P., 2004. Empirical mode decomposition as a filter bank. Signal Process. Lett. 11, 112–114.
Forbes, J.M., Leveroni, S., 1992. Quasi 16-day oscillation in the ionosphere. Geophys. Res. Lett. 19, 981–984.
Gillet, N., Jault, D., Canet, E., Fournier, A., 2010. Fast torsional waves and strong magnetic field within the Earth's core. Nature 465, 74–77.
Gillet, N., Jault, D., Finlay, C.C., Olsen, N., 2013. Stochastic modeling of the Earth's magnetic field: inversion for covariances over the observatory era. Geochem. Geophys. Geosyst. 14, 766–786.
Glassmeier, K.-H., 1980. Magnetometer array observations of a giant pulsation event. J. Geophys. 48, 127–138.
Glassmeier, K.-H., Auster, H.-U., Motschmann, U., 2007. A feedback dynamo generating Mercury's magnetic field. Geophys. Res. Lett. 34.
Hale, G.E., Nicholson, S.B., 1938. Magnetic Observations of Sunspots, 1917–1924. Carnegie Institution of Washington, Washington, D.C.
Heyner, D., Wicht, J., Gòmez-Pérez, N., Schmitt, D., Auster, H.-U., Glassmeier, K.-H., 2011. Evidence from numerical experiments for a feedback dynamo generating Mercury's magnetic field. Science 334, 1690–1693.
Hirooka, T., Hirota, I., 1985. Normal mode Rossby waves observed in the upper stratosphere. Part II: second antisymmetric and symmetric modes of zonal wavenumbers 1 and 2. J. Atmos. Sci. 46, 535–548.
Hirota, I., Hirooka, T., 1984. Normal mode Rossby waves observed in the upper stratosphere. Part I: first symmetric modes of zonal wavenumbers 1 and 2. J. Atmos. Sci. 41, 1253–1267.
Huang, N.E., Shen, Z., Long, S.R., Wu, M.C., Shih, H.H., Zheng, Q., Yen, N.-C., Tung, C. C., Liu, H.H., 1998. The empirical mode decomposition and the Hilbert spectrum for nonlinear and non-stationary time series analysis. Proc. R. Soc. 454, 903–995.
Jackson, A., Jonkers, A.R.T., Walker, M.R., 2000. Four centuries of geomagnetic secular variation from historical records. Philos. Trans. R. Soc. A: Math. Phys. Eng. Sci. 358, 957–990.
Jackson, L.P., Mound, J.E., 2010. Geomagnetic variation on decadal time scales: What can we learn from Empirical Mode Decomposition?. Geophys. Res. Lett. 37, L14307.
Jarvis, M., 2006. Planetary wave trends in the lower thermosphere—evidence for 22-year solar modulation of the quasi 5-day wave. J. Atmos. Solar-Terr. Phys. 68, 1902–1912.
Jault, D., Légaut, G., 2005. Alfvén waves within the Earth's core. In: Soward, A.M., Jones, C.A., Hughes, D.W., Weiss, N.O. (Eds.), Fluid Dynamics and Dynamos in Astrophysics and Geophysics, p. 277.
Kohsiek, A., Glassmeier, K., Hirooka, T., 1995. Periods of planetary waves in geomagnetic variations. Ann. Geophys. 13 (2), 168–176.
Labitzke, K., Matthes, K., 2003. Eleven-year solar cycle variations in the atmosphere: observations, mechanisms and models. The Holocene 13, 311–317.
Légaut, G., Jault, D., 2004. Torsional Alfvén waves excited inside the Earth's core because of modulations by the solar cycle of the electrical currents flowing in the magnetosphere. In: AGU Fall Meeting Abstracts, A871, December.
Lockwood, M., Nevanlinna, H., Barnard, L., Owens, M.J., Harrison, R.G., Rouillard, A. P., Scott, C.J., 2014. Reconstruction of geomagnetic activity and near-Earth interplanetary conditions over the past 167 yr—Part 4: near-Earth solar wind speed, IMF, and open solar flux. Ann. Geophys. 32 (April), 383–399.
Love, J.J., Rigler, E.J., 2014. The magnetic tides of Honolulu. Geophys. J. Int. 197, 1335–1353.
Lühr, H., Maus, S., 2010. Solar cycle dependence of quiet-time magnetospheric currents and a model of their near-Earth magnetic fields. Earth Planets Space 62, 843–848.
Malin, S., Hodder, B., 1982. Was the 1970 geomagnetic jerk of internal or external origin? Nature 296, 726–728.
Michelis, P.D., 2005. Geomagnetic jerks: observation and theoretical modeling. Mem. Soc. Astron. Ital. 76, 957–960.
Panovska, S., Finlay, C.C., Hirt, A.M., 2013. Observed periodicities and the spectrum of field variations in Holocene magnetic records. Earth Planet. Sci. Lett. 379, 88–94.
Parish, H.F., Forbes, J.M., Kamalabadi, F., 1994. Planetary wave and solar emission signatures in the equatorial electrojet. J. Geophys. Res.: Space Phys. 99, 355–368.
Pinheiro, K.J., Jackson, A., Finlay, C.C., 2011. Measurements and uncertainties of the occurrence time of the 1969, 1978, 1991, and 1999 geomagnetic jerks. Geochem. Geophys. Geosyst. 12.
Rilling, G., Flandrin, P., Gonçalvés, P., 2003. On empirical mode decomposition and its algorithms. In: Proceedings of the 6th IEEE/EURASIP Workshop on Nonlinear Signal and Image Processing.
Roberts, P.H., Yu, Z.J., Russell, C.T., 2007. On the 60-year signal from the core. Geophys. Astrophys. Fluid Dyn. 101 (February), 11–35.
Salby, M.L., 1984. Survey of planetary-scale traveling waves: the state of theory and observations. Rev. Geophys. 22, 209–236.
Velímský, J., Finlay, C.C., 2011. Effect of a metallic core on transient geomagnetic induction. Geochem. Geophys. Geosyst. 12, 1–8.
Wu, Z., Huang, N., 2009. Ensemble empirical mode decomposition: a noise-assisted data analysis method. Adv. Adapt. Data Anal. 1, 1–41.